Banknote Authentication with Mobile Devices

Volker Lohweg*[a], Jan Leif Hoffmann, Helene Dörksen[a], Roland Hildebrand, Eugen Gillich[a], Jürg Hofmann, and Johannes Schaede[b]

[a]inIT – Institute Industrial IT, Ostwestfalen-Lippe University of Applied Science, D-32657 Lemgo, Germany; [b]KBA-NotaSys S.A., CH-1018 Lausanne, Switzerland

ABSTRACT

Maintaining confidence in security documents, especially banknotes, is and remains a major concern for the central banks in order to maintain the stability of the economy around the world. In this paper we describe an image processing and pattern recognition approach which is based on the *Sound-of-Intaglio* principle for the usage in smart devices such as smartphones. Today, in many world regions smartphones are in use. These devices become more and more computing units, equipped with resource-limited, but effective CPUs, cameras with illumination, and flexible operating systems. Hence, it is obvious to apply smartphones for banknote authentication, especially for visually impaired persons. Our approach shows that those devices are capable of processing data under the constraints of image quality and processing power. Strictly a mobile device as such is not an industrial product for harsh environments, but it is possible to use mobile devices for banknote authentication. The concept is based on a new strategy for constructing adaptive Wavelets for the analysis of different print patterns on a banknote. Furthermore, a banknote specific feature vector is generated which describes an authentic banknote effectively under various illumination conditions. A multi-stage Linear-discriminant-analysis classifier generates stable and reliable output.

Keywords: Banknote, Authentication, Mobile Device, smartphone, Wavelet Transform, Classification, Adaptation, Sound-of-Intaglio

1. INTRODUCTION

Maintaining confidence in security documents, especially banknotes, is and remains a major concern for the central banks in order to maintain the stability of the economy around the world. Our approach is based on the recently introduced *Sound-of-Intaglio* approach, cf. [1, 2], which focuses on the analysis of intrinsic features produced by Intaglio printing. The result is a universal algorithm, based on image processing and pattern recognition which detects intrinsic information to distinguish between banknotes with genuine Intaglio, regardless of mint or worn out conditions, or even counterfeits. This is because Intaglio printing enables the printing of very fine, high resolution and sharply-defined patterns. Also, Intaglio is the most resistant printed feature which gives the methodology a certain advantage in robustness under the conditions of circulation. Therefore, Intaglio is identified "as it is" as an intrinsic feature and can serve as a secure method of identification for the public. The vast majority of counterfeits retrieved by police forces and banks are created with methods and equipment which are commercially available. Intaglio has proved to be the most reliable and secure platform for defence against counterfeits. Though Intaglio features are not consciously recognized by the public, the unmistaken optical appearance in combination with the unique tactile properties (both to be seen in combination with the printing substrate) is the key to the habitual recognition of genuine notes for the users. Our method identifies the unique features of Intaglio with affordable image analysis tools by using e.g. mobile telephones. Of course, the general approach can also be useful for central banks in sorting and forensics. Furthermore, an advantage of the concept is that there is no need for the central banks to disclose any secret information like special properties, geometries etc. and specifically no need to re-design existing banknotes, provided that the Intaglio reaches a certain quality level. Additionally, Intaglio represents one of the important differentiations to commercial prints and is a substantial part of the printing process of banknotes. The research focuses actually on the possibility of using Intaglio for automated applications in the cash cycle. For this reason, Sound-of-Intaglio offers a future frame for manufacturers of payment terminals or banking systems to secure the gap ahead and against the increasing quality of counterfeits in circulation. So far, the counterfeit technologies are unsuccessful in providing acceptable simulations of Intaglio or even to use the technology for criminal purpose.

*volker.lohweg@hs-owl.de, phone: +49 5261 702 408, fax: +49 5261 702 312

Volker Lohweg ; Jan Leif Hoffmann ; Helene Dörksen ; Roland Hildebrand ; Eugen Gillich ; Jürg Hofmann ; Johannes Schaede
Media Watermarking, Security, and Forensics 2013, Adnan M. Alattar; Nasir D. Memon; Chad D. Heitzenrater, Burlingame, California, USA | February 03, 2013

In addition to the "proved" mass counterfeits on commercial offset presses, the continuous progress in digital desktop technologies (scanners, cameras, and digital office printers) has established a complete new class of "digital" counterfeits (*digifeits*). Due to the strict non-proliferation policy in the printing industry, the high definition banknote Intaglio process in its totality (design, origination, plate making and printing) is well protected against its use or abuse in counterfeit applications. With the uniqueness of the Intaglio process for the security of banknotes, its unmistakable appearance and the function in public circulation, it is obvious to directly identify genuine banknotes by identifying the presence of Intaglio. As the direct measurement of 3D-structures under the rough and challenging conditions of circulation have proved to be difficult and lacking robustness, a complete different approach has been sought, which exploits the unique opacity and appearance of common high quality Intaglio structures.

In this paper we describe an image processing and pattern recognition approach which is based on the *Sound-of-Intaglio* approach [1] for the usage in smart devices such as smartphones [4] and others [3]. The concept is based on a new strategy for constructing adaptive Wavelets for the analysis of different print patterns on a banknote. Furthermore, a banknote specific feature vector is generated which describes an authentic banknote effectively under various illumination conditions. A multi-stage Linear-discriminant-analysis classifier generates stable and reliable output.

The paper is organized as follows: After the introduction, related work and prerequisites will be highlighted in the second section, where we focus on related papers, some technology aspects of mobile devices, and Wavelet-based Intaglio detection. In the third section our adaptive Wavelet approach on banknote authentication for smartphones will be pointed out. The fourth section is dedicated to results, and the fifth section concludes the paper and gives an outlook to the future work.

2. RELATED WORK AND PREREQUISITES

2.1 Related papers

In the last ten years several papers regarding the detection of banknote denominations and authentication as such are published. Not more than approx. 300 papers are detected in the SPIE, IEEE, and ACM databases during the above mentioned years. Most of the papers describe optical scanning techniques and signal processing algorithms in their approaches. Only a few authors suggest other than optical concepts, e.g. [5, 6]. The vast majority of published work is related to feature extraction and machine learning, e.g. [7, 8, and 9]. Some recent papers have also shown that a Wavelet approach seems to be promising in identification [10] and recognition [11] of banknote denominations. Especially, Wavelet-based concepts support our published general approach from 2007 [1] and underlining Wavelet-based authentication theory [12].

2.2 Mobile device technology

In this section, we describe key components of mobile devices, especially key components of state-of-art-smartphones. The focus is on the camera module, because this is the smartphone's key element if used as an image processing device.

Definition. A mobile phone is called a smartphone if it has the capability to be extended with small software applications (apps) and if it offers a more advanced computing ability and enhanced connectivity [13]. The increasing processor performance in recent years led to a hugely shifting usage behavior: At the beginning, smartphones were used to e-mail or to text in a more convenient way, mainly by business users. Today, smartphones can run third-party apps, which extend the functionality by far. The smartphone is not only a mobile telephone, but also a notebook, compact camera, gaming companion, music player, internet surf station, satellite navigation tool and so on. The most important market players use essentially two different operating systems: Apple iOS and Google Android. They share 86.3 % [14] of all smartphones in the field, sold worldwide in the third Quarter 2012, with Android being the biggest player with a market share of 72.4 % [14].

General Hardware. Usually, smartphones are equipped with a large display. Since the advent of Apple's iPhone in 2007, large high-resolution multi-touch displays have become a de-facto standard. The highest resolution (326-pixel-per-inch-display) is offered by Apple [15]. The Samsung Galaxy Note N7000, one of the largest smartphones currently on the market, is equipped with a screen size of 5.3 inch [16]. Furthermore, smartphones have a broad collection of sensors, e.g. gyroscope, accelerometer, GPS, proximity or light. The first smartphones used a single core processing unit with a

Volker Lohweg ; Jan Leif Hoffmann ; Helene Dörksen ; Roland Hildebrand ; Eugen Gillich ; Jürg Hofmann ; Johannes Schaede

clock rate of 600 MHz. Yet today, multi-core processors (four to five cores) and clock rates of about 1.5 GHz are built in high sophisticated models [17, 18]. A Smartphone usually has two cameras which are described in the next paragraph.

Camera unit. Typical smartphones employ two different types of cameras: one at the screen side for video phone calls, and one on the back. Usually, the first one has a resolution of about one Megapixel, the latter offers a higher sensor resolution and is designed to be a replacement for a still or video camera. Since this is the camera for applications in image processing, we use the term camera henceforth for high-resolution cameras and neglect the other one. A typical smartphone camera has a resolution between five and twelve Megapixels, with a trend to a larger amount of pixels. As with other compact cameras with low-quality optics, it does not mean that the result improves. Camera modules in smartphones lack a zoom lens (niche models like *Nokia Pureview 808* are ignored at this point). These cameras have a sensor with a diagonal width of 4 to 7 mm, which makes them prone to noise. The built-in illumination, often a LED- or Xenon-based flash, is only capable to illuminate objects near to the lens, e.g. portraits or close-ups.

Large resolution leads to large memory demand. Today, this is why it is not possible to get raw image data, which is important in image processing. The result of an image capturing process is always a jpg-compressed picture. However, it can be said that in general the compression factor is decreasing based on the state-of-art of smartphone technology.

2.3 Banknote applications for mobile devices

The vision of using mobile devices for banknote authentication is not new as such. Different papers have cited such kind of applications, e.g. [3, 4, and 19]. The basic idea is to use the integrated camera, the illumination unit, and the processing unit to analyse different overt and covert banknote features and to classify the banknotes. Another approach was recently published which is based on a pocket scanner equipped with optical near infrared point light sources and a low power sensor chip. This system can be connected to any mobile phone [20]. The technology imitates some of the basic concepts of ATM manufacturers. Besides these apps some more exist which can be used as banknote presentation applications, e.g. [21, 22].

2.4 Wavelet-based Intaglio detection

Preferably, the decomposition of the image is carried out by performing digital signal processing techniques based on Wavelets. In this subsection the general concept of *Wavelet-based Intaglio Detection* (WBID) is described. For further details of the concept and variants we have to refer to the corresponding literature because of space limitations, cf. [1, 2, 3, 4, and 12]

Wavelets. A Wavelet is a mathematical function used to divide a given function or signal into different scale components. A Wavelet transform (or Wavelet transform) is the representation of the function or signal by Wavelets. Wavelet transforms have advantages over traditional Fourier transforms for representing functions and signals that have discontinuities and sharp peaks. According to the present approach, one in particular exploits the properties of so-called discrete Wavelet transforms (DWTs) as it will be discussed in the following. Wavelet theory will not be discussed in-depth in the present description as this theory is well-known and is extensively discussed and described in several textbooks on the subject. The interested reader may for instance refer to the cited books and papers about Wavelet theory [23, 24, 25, and 26].

To recognize local features, it is important that the signal transform is shift invariant. This means a signal shift by Δ samples may lead to a shift of scaling or detail coefficients, but not to a modification of their values. This property guarantees that a scale diagram does not depend on the selection of the zero point on a scale. Using the Fast Wavelet Transform (FWT), we lose the property due to its inherent sub-sampling. Consequently, Wavelet coefficients show a high dependency on signal shifts. By sub-sampling when progressing to the next transform scale, we also run the risk of forfeiting important information on edges. Hence, it is crucial to apply a signal transform that is *shift invariant*. To attain a shift invariant transform, it is self-evident to determine the transform without the sub-sampling of a signal $s[n]$. This condition is met by the shift-invariant Wavelet Transform (SWT) [27, 28]. For shifted, but otherwise identical signals, SWTs provide shifted, but identical Wavelet coefficients. As no sub-sampling is used a redundant signal representation is gained [27, 28]. For transforming two-dimensional banknote images into spectral descriptions, two one-dimensional transforms are applied [28]. This is valid because images can be interpreted as separable signals [25]. To transform a two-dimensional signal $\mathbf{x}$, the one-dimensional transform algorithm alternately on the image rows n and the image columns m are employed. This results in a square matrix $\mathbf{X}$ with the dimensions $(2n \times 2m)$:

Volker Lohweg ; Jan Leif Hoffmann ; Helene Dörksen ; Roland Hildebrand ; Eugen Gillich ; Jürg Hofmann ; Johannes Schaede

$$X = \begin{bmatrix} A_y \\ D_y \end{bmatrix} = \begin{bmatrix} A & cV \\ cH & cD \end{bmatrix} . \qquad (1)$$

Now, the Wavelet-transformed signal is divided into four sub-images: Scaling coefficients **A** (lowpass-filtered, φ) and vertical detail coefficients **cV** (bandpass-filtered, ψ) belonging to A_y, and horizontal as well as diagonal detail coefficients (**cA** and **cD,** bandpass-filtered, ψ) are comprised in D_y. The detail matrices **cV**, **cH**, and **cD** describe the same structure of the Wavelet-transformed signal of the image. In a second step the detail coefficients are combined to a general detail matrix **cG**

$$cG = \alpha \cdot (cV + cH + cD), \quad \alpha \in \mathbb{R} , \qquad (2)$$

with α being a scale factor which guarantees the same dynamic range for the scaling coefficients and the details coefficients, if necessary. With **cG** all recognized structure transitions are united in one matrix. Please note that one cannot retrieve the signal from the united detail coefficients **cG**. When authenticating banknotes, though, this aspect is irrelevant. To process a Wavelet Transform it is necessary to fit a Wavelet to the application. In general, good results are achieved with *Daubechies Wavelets* [23] with two vanishing moments (db2-Wavelet). These Wavelets are *in average* well suited for spectral analysis of fine Intaglio structures because of their compact support [12].

Classification. The use of moment-based statistical features of Wavelet coefficients is advantageous [3, 12, and 29]. In Figure 1 we show different greyscale frequency histograms of db2-SWT coefficients $H_n(p)$ based on a typical Intaglio line structure of a *Jules-Verne-specimen* (Figure 2). Specimen banknotes are archetype banknotes with genuine paper, inks, applications, etc., but have no value. The specimen banknotes, *Jules Verne* and *Flowerpower*, are designed and produced by KBA-NotaSys SA in Lausanne, Switzerland.

The complete banknote is shown in Figure 7a. It is intuitive that the greyscale frequency distribution of genuine banknotes differs considerably from forged ones.
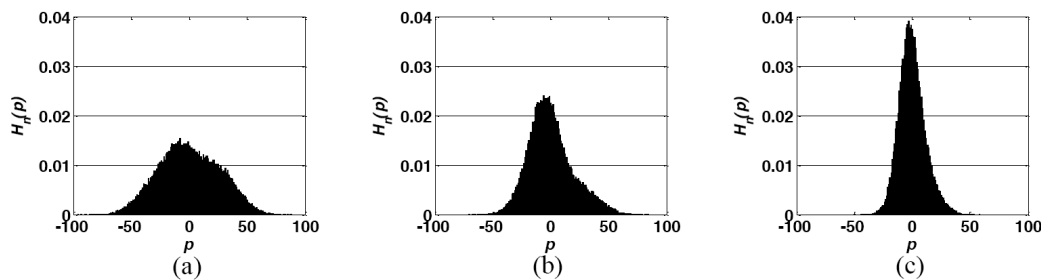

Figure 1. Histograms of Wavelet coefficients after a db2-SWT: Genuine (a), High-Quality Forgery (b), and Low-Quality Forgery (c). The greyscale frequency distribution of genuine banknotes differs considerably from forged ones [4].
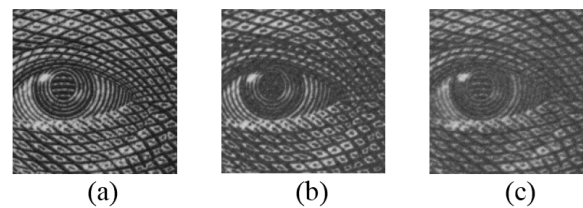

Figure 2. Intaglio line structures: Genuine (a), High-Quality Forgery (b), and Low-Quality Forgery (c) [4].

By calculating descriptive measures on standardized histograms $H_n(p)$ global conclusions on the image structure can be discussed. The following statistical features are taken into account for further analysis of the Wavelet coefficients: Variance σ^2 depicts the amplitude distribution of the Wavelet coefficients around the histogram center. Skewness E describes the symmetry of the distribution around the center. Excess C tells the deviation relative to the Gaussian distribution, cf. [29]. Figure 3 shows the feature space containing object classes which are to be classified.
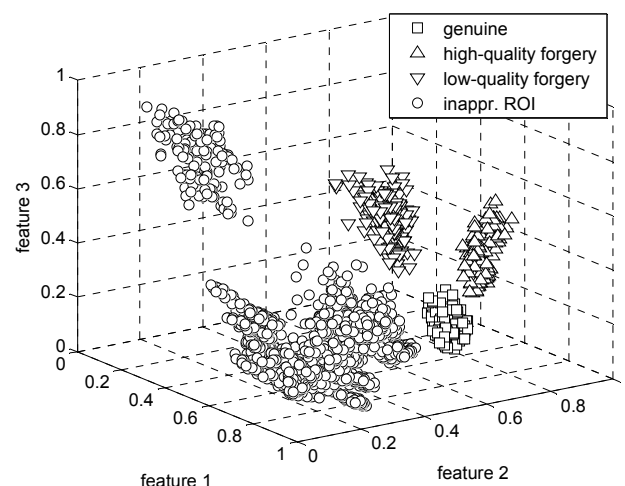
Volker Lohweg ; Jan Leif Hoffmann ; Helene Dörksen ; Roland Hildebrand ; Eugen Gillich ; Jürg Hofmann ; Johannes Schaede

Figure 3. Feature space – spanned over σ^2 (feature 1), E (feature 2), and C (feature 3). The training set consists of 1489 objects [29].

Generally, the well-known above mentioned features are not sufficient for discriminating a complex feature space uniquely. One has to keep in mind that not only newish, but worn out genuine and forged banknotes also have to be distinguished correctly. One approach to achieve a more accurate linear classification is to consider additional features. The additional features have to fulfil two important properties. First, they have to be *suitable for recognition of Intaglio printing, and second, they have to be complementary to the existing three statistical features*. We apply three typical statistical moments (variance σ^2, skewness E, and curtosis C). Three others, called LACH-features $\bar{H}_L$, $\bar{H}_M$ and $\bar{H}_R$ [4], have to be interpreted as *local adaptive cumulative histogram (LACH)* statistics which generate the features $\bar{H}_\mathbf{I}(\sigma^2), \mathbf{I} \in \{L, M, R\}$, controlled by the variance σ^2. They represent areas of the meaningful parts of the histogram, separated into parts using σ^2 (L for the left part, M for middle, R for right). Since most of the features are Gaussian distributed [4], we apply a *Linear Discriminant Analysis* (LDA) approach [4] for the calculation of the classifier boundary for the later authentication.

3. APPROACH

Our approach is based on the fact that signal processing algorithms for smartphones, if used as image processing units, have to fulfil some criteria regarding robustness and adaptivity. This section describes findings for robust and adaptable feature generation for Intaglio detection.

3.1 Robustness

By transferring authentication algorithms to a smartphone, the possible application areas are stretched, and the inspection of banknotes can be executed by untrained personnel. Implementing authentication algorithms on a smartphone demands a new concept for certain parts of some algorithms. Smartphone limitations that have, in this case, an effect are:

− quality fluctuations of the camera module,

− software limitations such as restricted or impeded access to raw image data,

− changing environmental conditions, esp. light conditions, and

− banknote position in respect to the smartphone's optics.

Camera modules in smartphones suffer from quality fluctuations during production. To reduce costs, such modules generate an already optimized image via special purpose hardware. The phone's operating system does not adjust on any deviation. Therefore, quality deviations caused by the camera module manufacturer lead to changing image quality. Mean quality can show itself in a color cast, i.e. the color channels are not properly adjusted, noise, bad focus

adjustment, and so on. These quality fluctuations have to be taken into account by an appropriate choice of algorithms. Several counter-measures try to compensate this, e.g. shading correction and white balance adjustment in post-processing steps. Shading correction compensates inhomogeneous illumination. White balance adjustment corrects color casts by adjusting the color channels to predefined reference values.

Use of a smartphone for real-time authentication of banknotes demands special procedures of machine learning. Classification of objects should be as robust as possible, despite of unstable capturing conditions. Furthermore, the application should be reliable, despite of a limited number of counterfeits for training. False-positive classifications have to be avoided. Therefore, a training set has to be designed which considers possible variations in the production process. When selecting an adequate classification method, it has to be taken into account that the number of counterfeits at hand is limited. The number of possible printing methods is also limited. Since false-positive classifications would question the whole application and lead to negative feedback in the public, the reliability of the classifier is most important. For this reason, the methods of machine learning which are used in the authentication process have to be well-considered.

3.2 Adaptive Wavelet approach

Banknote classification operates on statistical moments which are obtained from Wavelet coefficient histograms, which in turn are based on a db2-Wavelet transform of a given signal with a *typical resolution of 600 dpi*. Though this classification works well in many cases, in some it does not, i.e. misclassifications occur. Since the Intaglio printing technique is closely related to the Wavelet Transform [12], an adaptive Wavelet approach has to overcome such occurrences of misclassification. The approach is based on a Wavelet mapping for different Intaglio structures. The baseline is the db2-Wavelet which is replaced by another Wavelet type according to a certain local line structure of a banknote. We use Wavelets from the same Wavelet family (Daubechies [23]) or a Wavelet from a Wavelet family with other characteristics, e.g. *biorthogonal Wavelets*, *Coiflets* or *Symlets* [23, 24, and 25].

Our aim is a better ability to classify samples unambiguously. Therefore, prior to the Wavelet transform, we have to characterize a signal sample structure within a banknote and define a categorization map (C-map) for the whole banknote (cf. Figure 7b-7f). The C-map contains local information about the intaglio structure which is mapped to a certain Wavelet. Based on this categorization, it is possible to apply a Wavelet transform which generates quasi-optimal spatial frequency coefficients, and therefore, quasi-optimal detection features lead to an unambiguous classification.

For the approach, the essential steps can be divided into three parts: i) A *statistical model* is executed which works adequately for different given line structures; ii) a given sample structure has to be *measured* and distinguished; iii) a Wavelet has to be *selected* which fits best under the constraint of a limited Wavelet pool.

Statistical Model. The signal at hand is a 2D-raster image that can be regarded as two sets of 1D-signals, one horizontal and one vertical. For each dimension, first the centers of the edges (slopes) are determined. Secondly, two types of distances are calculated: The *line width w* which is the distance between the center of a falling and the center of a rising edge, and the *line distance d* which is the distance between the center of a rising and the center of a falling edge. This procedure is based on the underlying assumption that we inspect darker print structures on light, whitish cotton-based paper. Since we are using the centers of slopes as reference points, we are insensitive to the printing technique of the sample.

We are not interested in a single line or line distance, but in discrete statistical densities (histograms) regarding w and d for the whole observed structure. Hence, histograms of the measurements for w and d are calculated. Since the resulting densities have the appearance of the *Gamma probability density* $p(x;k,\theta)$ [30], parameter estimation for this distribution is executed. The Gamma probability density is defined as follows:

$$p(x;k,\theta) = \frac{1}{\theta^k}\frac{1}{\Gamma(k)}x^{k-1}e^{-\frac{x}{\theta}}; x,k,\theta \in \mathbb{R}_+ . \tag{3}$$

For a given variable x (here: w and d), the parameter estimation results in two parameters: shape k and scale θ. In our case, we observed that these two are strongly correlated, that is, $\theta = f(k)$. Hence, a histogram can be characterized by only one of them. The function $\Gamma(k)$ depicts the *Gamma function* [31]:

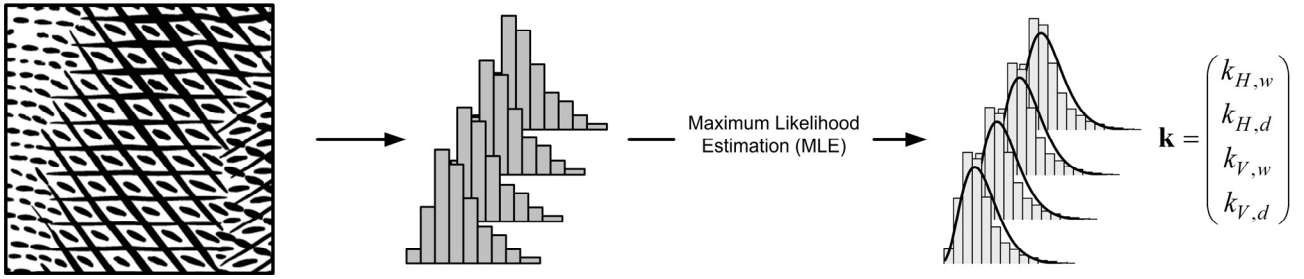$$\Gamma(k) = \int_0^\infty t^{k-1}e^{-t}dt .$$

Figure 4. Maximum Likelihood Estimation from a given Intaglio structure for horizontal and vertical line width and inter-line distance. The window size is typically set to 96×96 to 128×128 pixel, depending on the banknote structure, viz., line width and line distances.

We have chosen k, commonly known as shape parameter. For a given structure, the results form a characteristic 4-tuple $(k_{H,w}, k_{H,d}, k_{V,w}, k_{V,d})$, where H and V stand for horizontal and vertical direction of a measure, and w and d represent measurements of line width and distance, respectively. The estimation approach used here is based on *Maximum-Likelihood Estimation* (MLE) which is a standard method of estimation parameters of a statistical data's distribution or density [32]. Figure 4 represents the procedure.

Based on the above mentioned procedure different 4-tuples for prototype structures are generated. The prototype structures are based on typical banknote designs (horizontal lines, vertical lines, dashed lines, dotted lines, etc. aggregated to complex structures, cf. Figure 4). These prototypes are of course not unique for a banknote for two reasons i) a banknote is individually designed by the engraver with the creator's distinctive technique and ii) the designed regions are overlapped. These two observations lead to the fact that ambiguities in the 4-tuples occur. Therefore, a unique characterization of a region is not always possible. A best case situation appears if and only if:

$$\exists k_{\mathbf{I}} : \beta_l < k_{\mathbf{I}} < \beta_u \Leftrightarrow \exists k_{\mathbf{I}} : k_{\mathbf{I}} \in S_{\mathbf{I}}; \mathbf{I} \in \{H, w; H, d; V, w; V, d\} . \tag{4}$$

A parameter k_{I} of index set $\mathbb{I}$ is located between a lower border β_l and an upper border β_u. In this case, at least one k_{I} belongs to a set S_{I} of possible mappings for a certain Wavelet type. In all other cases a unique separation is not possible. Consequently, as we are interested in a general approach, a measurement and optimization phase has to follow.

Measurement. Standard smartphone camera units (8 to 12 Megapixel resolution) are sufficient for approx. 600 dpi resolution. A banknote or a part of it is imaged by a camera unit (here: mobile device) and divided in up to 360 (30×12) sub-images (cf. Figure 7) of the size 96×96 to 128×128 pixel with an overlap of an image quarter in each orientation. The sub-images are analysed regarding their line widths and distances properties and for each sub-image a 4-tuple $\mathbf{k}_j, j \in 0 \ldots 359$ is determined. Depending on $\mathbf{k}_j$ a certain Wavelet type is pre-selected a-priori.

Wavelet selection procedure. The selection is based on the finding that db2-Wavelets are able to act as feature generator for banknote authentication in general [1, 12, and 29]. However, some characteristic regions can not be handled by db2-Wavelets. Therefore, a pool of Wavelet types is selected to optimize the detection rate. Initially about 60 Wavelet types are considered in various experiments, resulting in a group of the following six $(\tau \in 0...5)$ selected Wavelets. We refer to Wasilewski's Wavelet Properties Browser [33] for details, viz., decomposition filter coefficients and sketches of various decomposition-filter impulse responses. The six Wavelets are selected on the principles of engraved Intaglio lines shapes and widths. The Wavelet filter length, $N = \mathrm{card}(\psi)$, is sorted in increasing order (cf. table 1). Therefore, the Wavelets's basis bandwidth in the frequency domain decreases accordingly.

The above mentioned Wavelets types (shape and size) are examined for best separation properties on different scales in a considered feature space. Therefore, the Wavelet type's pool is allocated to the C-map. The procedure is executed as follows: A set of genuine and forged banknotes (approx. 20-50 pieces) is used to create two clusters (classes: genuine (G) and forgery (F)) for each of six r-dimensional feature spaces $\mathbf{f}_\tau$, based on the Wavelet types, and for each of j sub-images. Via LDA which was already used for classification purposes in banknote authentication [4] a scalar discriminant measure for each of the Wavelet types, known as *Rayleigh coefficient* D_τ [34], is determined. The non-negative real Rayleigh coefficient, $0 \le D_\tau \le \infty$, provides information about the distance between two clusters in a feature space.

Table 1. Selected 1D-Wavelet types [33] for banknote authentication (DLP: Decomposition low-pass (scaling function φ), DBP: Decomposition band-pass ψ (Wavelet)).

τ	Type	Filter length N (DLP, DBP)	Properties
0	Daubechies-2 (db2)	4, 4	asymmetric, orthogonal; rough function; compact support
1	Reverse biorthogonal 3.1 (rbio3.1)	4, 4	symmetric, biorthogonal; use of decomposition filters; smooth function; linear phase; compact support
2	Daubechies-4 (db4)	8, 8	asymmetric, orthogonal; compact support
3	Reverse biorthogonal 5.5 (rbio3.1)	11, 9	symmetric, biorthogonal; use of decomposition filters; smooth function; linear phase; compact support
4	Symlet-5 (sym5)	10, 10	near symmetric, orthogonal, biorthogonal; compact support
5	Coiflet-2 (coif2)	12, 12	near symmetric, orthogonal, biorthogonal; compact support

The higher D_τ , the larger is the distance between two clusters. As a reference measure D_0 is applied (db2). In case of

$$\Sigma_\tau = \frac{D_\tau - D_0}{D_0} > 0,\ \tau \in \{1,...,5\}\ , \tag{5}$$

it is assumed that the *separation ability* Σ_τ of a certain Wavelet type , $\tau \neq 0$, is better in a sense of larger cluster distances in the feature space. In all other cases $(\Sigma_\tau \leq 0)$, the db2-Wavelet has to be applied. It has to be pointed out that the separation ability is dependent on the utilized features. The determination of the Rayleigh coefficient *for each of the sub-images and Wavelet types* is identified as follows: In a feature space **f**, consisting of three (dimension: $r = 3$) statistical moments (variance, skewness, curtosis) as features, calculated from spatial frequency histograms of each local region and Wavelet scale, we look for a direction $\mathbf{v} = (v_1, v_2, \ldots, v_r)^T$ representing linear combinations of the features which separates the class means optimally (when projected onto the found direction) while achieving the smallest possible variance around these means. The empirical class means for a one-dimensional feature space *f* of classes genuine *G* with *n* objects and forgery *F* with *m* objects are

$$m(G) = \frac{1}{n}\sum_{f \in G} f \tag{6}$$

and

$$m(F) = \frac{1}{m}\sum_{f \in F} f\ . \tag{7}$$

Similarly, the means of the data projected onto some direction **v** in a higher-dimensional feature space can be computed by

$$\mu(G) = \frac{1}{n}\sum_{\mathbf{f} \in G} \mathbf{v}^T\mathbf{f}\ , \tag{8}$$

and

$$\mu(F) = \frac{1}{m}\sum_{\mathbf{f} \in F} \mathbf{v}^T\mathbf{f}\ . \tag{9}$$

The variances $\sigma^2(G)$ and $\sigma^2(F)$ of the projected data can be expressed as

$$\sigma^2(G) = \sum_{\mathbf{f} \in G} \left(\mathbf{v}^T \mathbf{f} - \mu(G) \right)^2, \tag{10}$$

and

$$\sigma^2(F) = \sum_{\mathbf{f} \in F} \left(\mathbf{v}^T \mathbf{f} - \mu(F) \right)^2. \tag{11}$$

The LDA solution is the direction $\mathbf{v}^*$ which maximizes the optimization problem

$$D(\mathbf{v}^*) = \max_{\mathbf{v}} \frac{\left(\mu(G) - \mu(F) \right)^2}{\sigma^2(G) + \sigma^2(F)}. \tag{12}$$

Within the described direction $\mathbf{v} = \left(v_1, v_2, \ldots, v_r \right)^T$, representing a linear combination of the features, and

$$\mathbf{m}(G) = \left(\mu_1(G), \mu_2(G), \ldots, \mu_r(G) \right)^T, \mathbf{m}(F) = \left(\mu_1(F), \mu_2(F), \ldots, \mu_r(F) \right)^T,$$

Equation (12) is rewritten with the inter- and intra-class *co-variances*

$$\mathbf{S}_b = \left(\mathbf{m}(G) - \mathbf{m}(F) \right) \left(\mathbf{m}(G) - \mathbf{m}(F) \right)^T \tag{13}$$

and

$$\mathbf{S}_v = \frac{1}{n} \sum_{\mathbf{f} \in G} \left(\mathbf{f} - \mathbf{m}(G) \right) \left(\mathbf{f} - \mathbf{m}(G) \right)^T + \frac{1}{m} \sum_{\mathbf{f} \in F} \left(\mathbf{f} - \mathbf{m}(F) \right) \left(\mathbf{f} - \mathbf{m}(F) \right)^T \tag{14}$$

as

$$D(\mathbf{v}^*) = \max_{\mathbf{v}} \frac{\mathbf{v}^T \mathbf{S}_b \mathbf{v}}{\mathbf{v}^T \mathbf{S}_v \mathbf{v}}. \tag{15}$$

The adaption process is executed as follows: For each k-tuple $\mathbf{k}_j$ a Wavelet type τ is allocated based on the distance measure Σ_τ under the constraint that each $k_\mathbf{I}$ is in a range $\beta_l < k_\mathbf{I} < \beta_u$, resulting in an initial Wavelet assignment. Of course, the mapping is not in all cases complete and unique. However, the more banknote designs are analysed, the more the map will be complete. Ultimately, the C-map consists of a near-optimal mapping $\max \Sigma_\tau : \mathbf{k}_j \to \tau$ which is independent of a certain banknote design and denomination.

3.3 Luminance adapted classification

It was shown in [1, 4, and 12] that pattern recognition within industrial devices can be performed using Wavelet transform-based features. In spite of different environmental and hardware conditions and, respectively, different feature distributions, which appear by application of mobile devices, it was possible to prove in [4] that the same features are suitable for mobile use. Unfortunately, only under special restrictions the pattern recognition process from [4] in its original form is feasible for a real world application. One restriction is a rigid position of the camera during the authentication, another, the environmental dependence on the authentication result. Especially illumination plays an important role in the authentication process. The limitations in terms of a rigid position and illumination dependence stem from the training data set, which we used in [4]. Unfortunately, in this training data set we did not consider possible shifts of the banknote during authentication. Further, since the training data was collected under daylight and standard office illumination, authentication could cause problems in other environmental situations. These two unfavorable topics are reported by persons who are asked to perform tests with our application. Under consideration of these circumstances, we describe below how to construct a more sufficient training data set and an accurate classification boundary.

We shortly recap the pattern recognition process described in [4]. The recognition is based on the authentication of a rigid banknote region. For authentication the region is transformed into the Wavelet domain; then, six features are calculated by using the Wavelet coefficients histograms. Three of them are conventional statistical moments
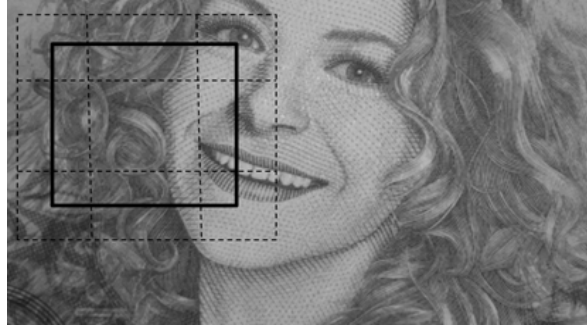
Figure 5. The detail shows one main region, which is used for the authentication (solid lines), and four further regions (dashed lines), which are added to the training data set (Specimen banknote KBA-NotaSys *Flowerpower*).

(variance σ^2, skewness E, and curtosis C). Three additional ones are called LACH-features $\bar{H}_L$, $\bar{H}_M$ and $\bar{H}_R$ (cf. section 2.4). Since most of the features are Gaussian distributed [4], we use once more LDA for the calculation of the classifier boundary for the later authentication. Furthermore, by applying our LDA strategy the training is fast, more flexible, and becomes more robust than using a Support Vector Machine (SVM). We refer to [29].

To overcome the problem of the rigid positioning in [4], we construct a more sufficient training data set by the following strategy: the training data set is extended by additional regions, which lie closely to the boundary of the main region. Figure 5 illustrates additional regions.

To overcome the illumination problem, we need to identify the features which are sensitive against luminance variations. For this reason we collect some data under several different illumination conditions. The validation of the feature distributions shows that the variance σ^2 is most likely sensitive against certain luminance variations, i.e. the distributions of σ^2 are not the same for the different luminance variations (the influence of the illumination on σ^2 is clarified by classification results in Figure 6 below). The other five features are less sensitive and possess similar distributions for different luminance variations. Within these results, it is more appropriate to construct a classification boundary by the combination of the five features, which are less sensitive against luminance variations. Since the variance σ^2 is an important feature for our application, it is used in classification as a stand-alone feature with large detection margin.

4. EXPERIMENTAL RESULTS

In this section we present actual results based on our findings. We use in our experimental design real banknotes (EURO banknotes) and specimen banknotes *Jules Verne* and *Flowerpower* which are produced in large volumes by KBA-NotaSys as genuine notes and different types of forged notes. For obvious reasons we do not describe the forging process here.

In Figure 6 the maximum likelihood estimation of a sub-image $(j = 47)$ on the forehead of Jules Verne (cf. Figure 7a) is exemplified. The black curve represents the best possible Gamma probability density for *vertical line widths* in the region with the parameters $k_{V,w} = 5.97$ and $\theta_{V,w} = 0.9$. Parts of the forehead Intaglio structures generate sub-image densities within the same range regarding their parameters. The analysis (cf. Figure 7c) results in a 4-tuple where simply two parameters control the forehead region regarding a certain Wavelet uniquely: Daubechies-4-Wavelets. As $k_{H,w} \geq 7.2$ and $k_{V,w} \geq 5.8$ are determined, the lower border parameters β_l are set to $\beta_{l;H,w} = 7.2$ and $\beta_{l;V,w} = 5.8$. The border upper border parameters β_u are set to $\beta_{u;H,w} = 10$ and $\beta_{u;V,w} = 8$ which defines half of the maximum frequency $h(d)$ and $h(w)$. Therefore: $7.2 < k_{H,w} < 10$ and $5.8 < k_{V,w} < 8$. The structure is modelled with an eight coefficient Wavelet with a maximum distance measure in the feature space: $\arg\max_\tau \Sigma_\tau = 2$. In this case the best Wavelet can be chosen with two parameters. Figure 7c exhibits the results for sub-images in question. For instance, the db4-Wavelet is able to distinguish better between a genuine and a forged banknote (up to 61%) compared to the db2-Wavelet in sub-image 47. As depicted in Figures 7b, 7d, 7e, and 7f different Wavelet types are able to distinguish different Intaglio regions (e.g. $j = 257$, 44 % with sym5-Wavelet).
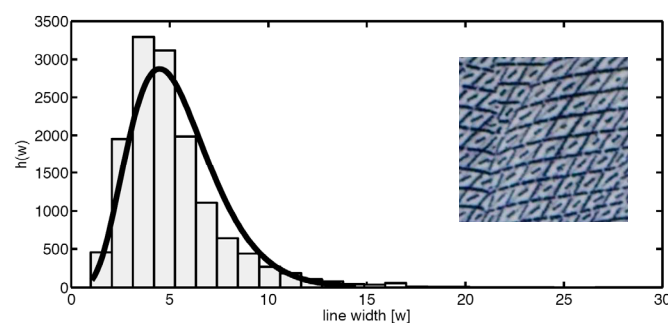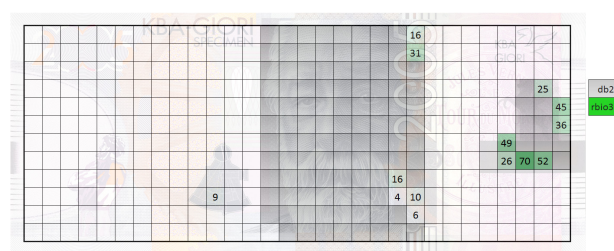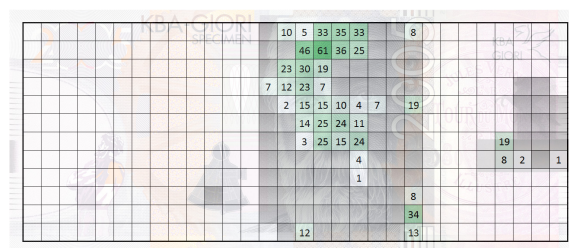
Figure 6. Maximum Likelihood Estimation from a given Intaglio structure for horizontal and vertical line width in pixel (region j = 47, forehead, specimen banknote *Jules Verne*; cf. Figure 7a). Counting of the sub-images j begins at the upper left edge in row direction, cf. e.g. Figure 7c.
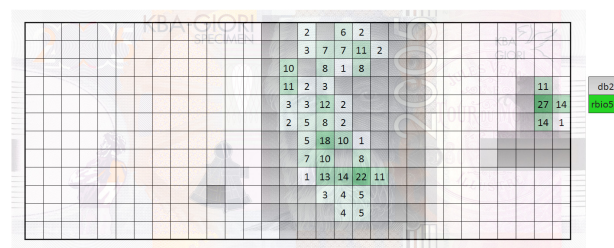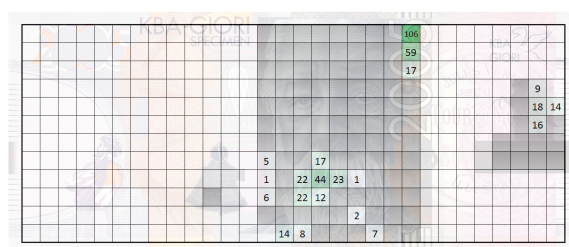

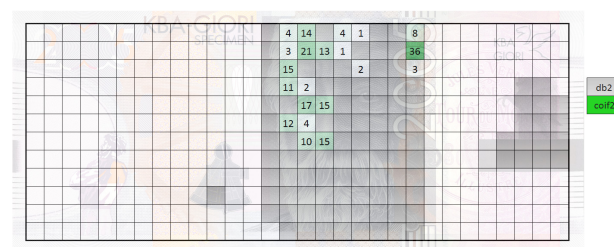Figure 7. In (a) a specimen banknote KBA-NotaSys *Jules Verne* is shown. The images (b)-(f) represent the results of different Wavelet feature generators compared to the db2-Wavelet. All values are denoted in %. The grayish sub-images are analysed regarding Intaglio print. No percentage values represent the separation ability of the db2-Wavelet (0% improvement). Percentage values show the improvements per sub-image related to a certain Wavelet type; (b): rbio3.1, (c): db4, (d): rbio5.5, (e): sym5, (f): coif2. Counting of the sub-images j begins at the upper left edge in row direction.

In the case of illumination variations (A and B (reduced luminance by approx. 30%)), there would be no need to change the classification strategy represented in [4]. However, by the modification of the training data set against rigid positioning, the classification rule has also to be modified. Since the extended training data set is not Gaussian any more,

the accuracy of the classification could be doubted. Special problem zones are regions, which lie closely to the classification boundary. We solve this problem by multi-stage LDA performed on the objects around the classification boundary. The comparison of results is illustrated in Figure 8 (original classification from [4].) and in Figure 9 (improved approach). We refer to a *video* which shows an application on banknote authentication via a *Sony Ericsson arc* smartphone [35].
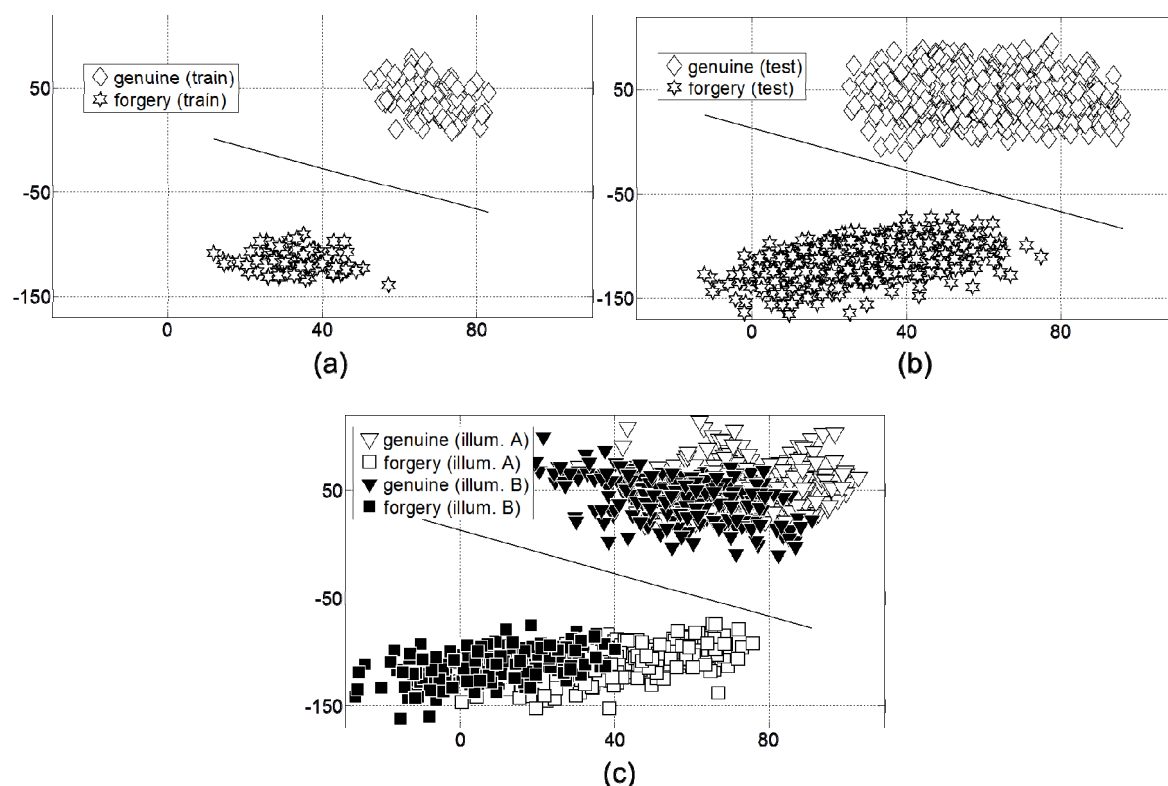

Figure 8. (a) shows the original LDA training from [4] for the data set collected by rigid positioning of the camera with respect to the banknote. In (b) the test data set based on additional regions (cf. Figure 5) and the same illumination as the training data set is presented. Here, some genuine objects move too close to the classification boundary which is inconvenient for our application. In (c) the same test data set with two different illuminations (type A and type B (reduced luminance by approx. 30%)) is shown. The distributions for illuminations A and B do not coincide. Moreover, some forgery objects move too close to the classification boundary which is crucial for our application. If a single forgery object is classified as a genuine one, it can then lead to a negative feed-back on the whole application.
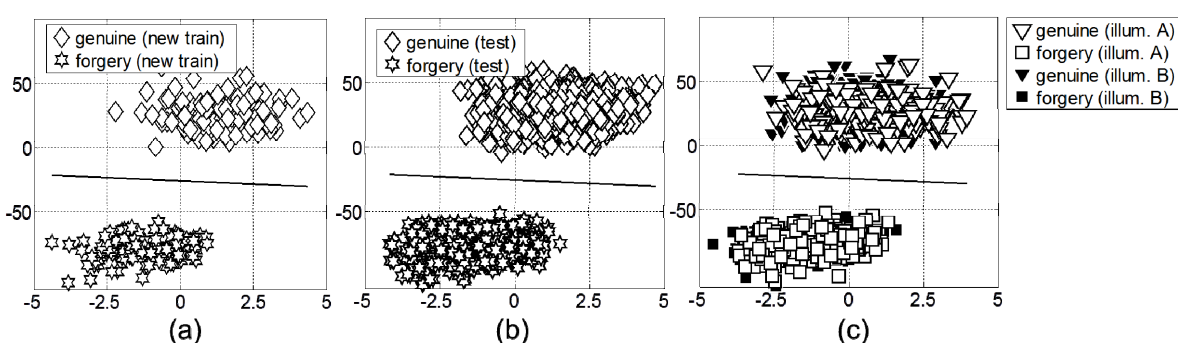

Figure 9. (a) shows a classification boundary with an improved approach. In (b) and (c) the same data sets as in Figure 8 are illustrated. In this approach the test objects do not move close to the classification boundary. Moreover, distributions coincide for illumination A and B. Hence, a higher stability against shifted positioning of the camera and different illuminations is achieved here.

Volker Lohweg ; Jan Leif Hoffmann ; Helene Dörksen ; Roland Hildebrand ; Eugen Gillich ; Jürg Hofmann ; Johannes Schaede

5. CONCLUSION AND FUTURE WORK

This section concludes the results and gives an outlook to future work and findings regarding banknote authentication by Sound-of-Intaglio.

5.1 Conclusion

The Sound-of-Intaglio approach is well suited for different applications in banknote production and authentication, namely quality inspection, sorting and authentication at different levels. We have shown that the general authentication approach can be optimized by adaption of the feature generators in question, namely the usage of a pool of Wavelets which are optimized for different Intaglio strutcures. Furthermore, by taking into account a border surrounding of each analysis region and adaption of the used features [4], luminance variations can be stabilized. Therefore, a more robust classification between genuine and forged banknotes is achieved.

5.2 Future work

Currently, further research on correlation between the 4-tuples to Wavelets on the basis of various Intaglio structures is executed. Especially, more investigations are necessary regarding the modeling of generic Intaglio pattern and a unique mapping between pattern and optimized Wavelets. Furthermore, research regarding illumination and optical positioning robustness will be carried out.

ACKNOWLEDGEMENTS

REFERENCES

[1] Lohweg, V., Gillich, E., Schaede, J., "Authentication of Security Documents, in Particular of Banknotes," Pat. EP2000992 Prio 2007-06-01, (2010).

[2] Lohweg, V., "Renaissance of Intaglio," Keesing Journal of Documents & Identity, Keesing Reference Systems Publ. 33, 35-41 (2010).

[3] Lohweg, V. and Schaede, J., "Document Production and Verification by Optimization of Feature Platform Exploitation," Optical Document Security - The Conference on Optical Security and Counterfeit Detection II San Francisco CA USA, 1-15 (2010).

[4] Lohweg, V., Dörksen, H., Gillich, E., Hildebrand, R., Hoffmann, J. L., Schaede, J., "Mobile Devices for Banknote Authentication – is it possible?," Optical Document Security - The Conference on Optical Security and Counterfeit Detection III San Francisco CA USA, 1-15 (2012).

[5] Gan, T.H., Hutchins, D. A., Billson, D. R., Schindel, D. W., "High resolution air-coupled ultrasonic imaging of thin materials," IEEE ULTRASONICS SYMPOSIUM, 897-990 (2002).

[6] Yang, C-N., Chen, J-R., Chiu, C-Y., Wu, G-C., Wu, C-C., "Enhancing Privacy and Security in RFID-Enabled Banknotes," IEEE International Symposium on Parallel and Distributed Processing with Applications, 439-444 (2009).

[7] Ahmadi, A., Omatu, S., Kosaka, T., "Improvement of the reliability of bank note classifier machines," Proc. IEEE International Joint Conference on Neural Networks 2 doi: 10.1109/IJCNN.2004.1380134, 1313-1316 (2004).

[8] Omatu, S., Yoshioka, M., Kosaka, Y., "Bank note classification using neural networks," IEEE Conference on Emerging Technologies and Factory Automation doi: 10.1109/EFTA.2007.4416797, 413-417 (2007).

[9] Shan, G., Peng, L. Jiafeng, L., Xianglong, T., "The design of HMM-based banknote recognition system," IEEE International Conference on Intelligent Computing and Intelligent Systems 4 doi: 10.1109/ICICISYS.2009.5357719, 106-110 (2009).

[10] Choi, E., Lee, J., Yoon, J., "Feature Extraction for Bank Note Classification Using Wavelet Transform," 18th International Conference on Pattern Recognition 2 doi: 10.1109/ICPR.2006.553, 934-937 (2006).

[11] Ahangaryan, F.P., Mohammadpour, T., Kianisarkaleh, A., "Persian Banknote Recognition Using Wavelet and Neural Network," International Conference on Computer Science and Electronics Engineering (ICCSEE) 3 doi: 10.1109/ICCSEE.2012.294, 679-684 (2012).

[12] Glock, S., Gillich, E., Schaede, J., Lohweg V., "Feature Extraction Algorithm for Banknote Textures based on Incomplete Shift Invariant Wavelet Packet Transform," Proceedings of the 31st DAGM Symposium on Pattern Recognition, Lecture Notes on Computer Science 5748, 422-431 (2009).

[13] Bezboruah, T., "Mobile computing: the emerging technology, sensing, challenges and applications," Preprint, <http://users.ictp.it/~pub_off/preprints-sources/2010/IC2010102P.pdf> (01 December 2012). http://users.ictp.it/~pub_off/preprints-sources/2010/IC2010102P.pdf

[14] Pettey, C. and van der Meulen, R., "Gartner Says Worldwide Sales of Mobile Phones Declined 3 Percent in Third Quarter of 2012; Smartphone Sales Increased 47 Percent," 2012, <http://www.gartner.com/it/page.jsp?id=2237315> (30 December 2012). http://www.gartner.com/it/page.jsp?id=2237315

[15] Apple, "iPhone features," 2012, <https://www.apple.com/iphone/features/> (30 December 2012). https://www.apple.com/iphone/features/

[16] Samsung, "Galaxy N7000," 2012, <http://www.samsung.com> (30 December 2012). http://www.samsung.com

[17] AnTuTu, "Benchmark-Tool Antutu," 2012, <http://www.Antutu.com/> (30 December 2012). http://www.Antutu.com/

[18] SunSpider, "Benchmark-Tool SunSpider 0.9.1," 2012, <http://www.webkit.org/perf/sunspider/sunspider.html> (30 December 2012). http://www.webkit.org/perf/sunspider/sunspider.html

[19] de Heij, H.A.M., "Public Feedback for better Banknotes Design 2," DNB Occasional Studies 5(2) De Nederlandsche Bank NV, (2007).

[20] Fake Currency Doctors, "Banknote Authentication," 2012 <http://voicendata.ciol.com/content/service_provider/110020318.asp> (01 December 2012). http://voicendata.ciol.com/content/service_provider/110020318.asp

[21] Illés, L., "iValuta," 2012 <http://itunes.apple.com/us/app/ivaluta/id327705750?mt=8> (01 December 2012). http://itunes.apple.com/us/app/ivaluta/id327705750?mt=8

[22] Macsoftex, "All Dollars," 2012 <http://itunes.apple.com/tw/app/all-dollars/id341552027?mt=8> (01 December 2012). http://itunes.apple.com/tw/app/all-dollars/id341552027?mt=8

[23] Daubechies, I., [Ten Lectures on Wavelets], CBMS-NSF Regional Conference Series in Applied Mathematics 61 SIAM (Society for Industrial and Applied Mathematics), Philadelphia, 1992.

[24] Burrus, S. C., Gopinath, R. A., Guo, H., [Introduction to Wavelets and Wavelet Transforms: A Primer], Prentice-Hall, Upper Saddle River, 1998.

[25] Walnut, D. F., [An Introduction to Wavelet Analysis], Birkhäuser, Boston, 2004.

[26] Mallat, S. G., "A Theory for Multiresolution Signal Decomposition: The Wavelet Representation," IEEE Transactions on Pattern Analysis and Machine Intelligence 11(7), 674-693 (1989).

[27] Pesquet, J. C., Krim, H., Carfantan, H., "Time-invariant orthonormal Wavelet representations," IEEE transactions on signal processing 8, 1964-1970 (1996).

[28] Fowler, J. E., "The redundant discrete Wavelet transform and additive noise," IEEE Signal Processing Letters 9, 629-632, (2005).

[29] Gillich, E., Lohweg, V., "Banknote Authentication," 1. Jahreskolloquium Bildverarbeitung in der Automation ISBN 978-3-9814062-0-7 Institute Industrial IT, 1-8 (2010).

[30] Hogg, R. V. and Craig, A. T., [Introduction to Mathematical Statistics], Macmillan New York, Sec. 3.3 (1978).

[31] Whittaker, E. T. and Watson, G. N., [The Gamma function], Cambridge University Press, 235–264 (1996).

[32] Chambers, R. L., Steel, D. G., Wang, S., [Maximum Likelihood Estimation for Sample Surveys], CRC Press Boca Raton, (2012).

[33] Wasilewski, F., "PyWavelets," 2008-2012, <http://Wavelets.pybytes.com/> (01 December 2012). Wavelets.pybytes.com

[34] Horn, R. A. and C. A. Johnson, [Matrix Analysis], Cambridge University Press, 176–180 (1985).

[35] Lohweg, V., "Mobile Sound-of-Intaglio," 2007-2012, <http://www.hs-owl.de/init/en/research/projects/b/filteroff/21/single.html> (1 December 2012). http://www.hs-owl.de/init/en/research/projects/b/filteroff/21/single.html